 doi:10.20944/preprints202102.0505.v1

Article

Adsorption of Polymer-Grafted Nanoparticles on Curved Surfaces

Aye Ozmaian[1], Rob D. Coalson[2], Masoumeh Ozmaian[3,*]

[1] Department of Neuroscience, University of Alberta, Edmonton, AL T6G 2R3, Canada
[2] Department of Chemistry, University of Pittsburgh, Pittsburgh, PA 15260, United States
[3] Department of Chemistry, University of Texas at Austin, Austin, TX 78712, United States
* Correspondence: ozmaian@utexas.edu

Abstract: Nanometer-curved surfaces are abundant in biological systems as well as in nano-sized technologies. Properly functionalized polymer-grafted nanoparticles (PGNs) adhere to surfaces with different geometries and curvatures. This work explores some of the energetic and mechanical characteristics of the adhesion of PGNs to surfaces with positive, negative and zero curvatures using Coarse-Grained Molecular Dynamics (CGMD) simulations. Our calculated free energies of binding of the PGN to the curved and flat surfaces as a function of separation distance show that curvature of the surfaces critically impacts the adhesion strength. We find that the flat surface is the most adhesive, and the concave surface is the least adhesive surface. This somewhat counterintuitive finding suggests that while a bare nanoparticle is more likely to adhere to a positively curved surface than a flat surface, grafting polymer chains to the nanoparticle surface inverts this behavior. Moreover, we studied the rheological behavior of PGN upon separation from the flat and curved surfaces under external pulling force. The results presented herein can be exploited in drug delivery and self-assembly applications.

Keywords: adhesion; self-assembly; drug delivery; curved surface; template-assisted self-assembly; nanotechnology; single-molecule system; polymer nanocomposite.

1. Introduction

Polymer nanocomposites are an important class of material with numerous applications[1-3]. Chemical versatility has made polymers good candidates to enhance the physiochemical properties of nanoparticles. Among different combination of polymers and nanoparticles in polymer nanocomposites, the polymer-grafted nanoparticles (PGNs) motif can be exploited in a wide variety of applications such as Janus particles, drug delivery systems and self-assembled structures[4-7]. This motif usually consists of a nanoparticle, as a spherical hard core, coated with polymeric chains that are tethered at one end. Grafted polymer chains are selected to either modify the chemical properties of the nanoparticles on the surface or their morphology and geometry. These modifications, for instance, can sterically stabilize a dispersion of nanoparticles and prevent their aggregation, or enable us to tailor the interaction of the nanoparticles with targeted surfaces[8-12]. Of particular relevance to this research area is controlling the adhesion of nanoparticles to different surfaces, which is a challenge in numerous applications[13, 14]. For instance, nanoparticles that are used in enhancing inflammation resolution during atherosclerosis need to bind to a curved endothelial layer during delivery[15]. The strength of this binding determines the effectiveness of the delivery. Another example is the colloidal probe technique, which uses a polymer-grafted colloidal particle attached to the end of a cantilever to measure the interaction forces between the colloidal particle and a surface[16]. The geometry of the surface is not limited to flat and smooth. Therefore, consideration of the effect of various curvatures on the interaction forces can help expand this technique to include various roughness and concave surfaces as well. However, only limited studies have been conducted to date on the adhesion of PGNs as a function of surface curvature[17-19].

Preprints (www.preprints.org) | NOT PEER-REVIEWED | Posted: 23 February 2021 doi:10.20944/preprints202102.0505.v1

Another aspect of our study focuses on its application in the self-assembly and synthesis of shape-controlled nanostructures[20-23]. It has been shown that surface roughness significantly influences attachment of colloids to the surface[24-26]. Based on this behavior, physical templates have been utilized to control the self-assembly of colloids into desired shapes[27, 28]. When a PGN is attached to a surface due to the attractive force, the mobile nature of the tethered polymer chains causes faster diffusion of the particle over the surface and steering it towards the global minimum state. Modifying the surface with controlled curvature elements can serve as a method for designing these global minima, and subsequently the organization of the nanoparticles on the surface. PGNs provide more flexibility in the assembly process as well as the capability to synthesize more complicated final structures. Furthermore, the liquid-like behavior of the tethered polymer chains results in a capillary attracting force between the nanoparticle and the surface, which is known as one of the main categories of the self-assembly techniques[29, 30].

Numerous experimental and theoretical studies have been performed on understanding the equilibrium as well as the transient behavior of PGNs[31-34]. Beside the chemical properties of the polymer chains, nanoparticle and the targeted surface, the size of the nanoparticle, polymer grafting density and polymer chain length are among the parameters that determine the surface adhesion properties of the PGN. In addition to the properties of the polymer grafted nanoparticles, the geometry and morphological properties of the surface onto which the particles are adsorbed also play an important role in the adhesion strength. In this study, we investigate the effect of surface curvature on the adhesion of a polymer grafted nanoparticle to the surface. The curvatures (essentially holes in and bumps on the surface) that we simulate, are about the size of the PGN. At this scale, and depending on the strength and the range of interaction potential, the surface geometry determines the amount of free space around the polymer chains and consequently the distribution of the polymer chains interacting with the surface. Our results show that among the three surfaces, the flat surface is the most energetically favorable surface that the PGN adheres to. In contrast, a bare nanoparticle is more likely to adhere to a concave surface, considering that it has a greater contact area compared to the flat and convex surfaces, as well as a lock and key geometry [28, 35].

This paper is organized as follows. First, we explain the coarse-grained molecular model and parameters we use to simulate our polymeric system. Results are discussed in the next section. We first investigate the free energy profile of the interaction between the PGN and the curved surfaces as a function of separation distance. This is followed by a discussion of the process of separation of the PGN from the convex, concave and flat surfaces under external pulling force. Finally, the numerical results are compared to the predicted values by the Johnson–Kendall–Roberts (JKR) theory that describes the adhesion mechanics of a deformable object on a rigid surface.

2. Method

Our coarse-grained model consists of bead-and-spring polymer chains placed in a solution with implicit solvent. The CGMD method is used to simulate the dynamics of the system[36].

Our system consists of a rigid spherical nanoparticle with radius $R_0 = 10\sigma$, which itself is a hollow shell consisting of 1020 smaller particles, possessing an excluded volume size corresponding to 1 monomer diameter. The nanoparticle is coated with 100 grafted polymer chains, randomly distributed over its surface. Each polymer chain has a chain length of $L_0 = 50\sigma$. The monomer of each polymer chain that connects to the nanoparticle is rigidly attached to a designated spot on the nanoparticle surface. The whole system is confined in a cubical box with the dimension of 100σ along each of its three dimensions. All the flat and curved surfaces are constructed out of spherical particles having the same diameter as that of a polymer monomer, close packed into a lattice one particle thick, and constrained in place during a simulation.

Preprints (www.preprints.org) | NOT PEER-REVIEWED | Posted: 23 February 2021 doi:10.20944/preprints202102.0505.v1

The specifics of the interactions in the system are as follows. The monomers of polymer chains as well as the particles that make up the nanoparticle are represented as beads of equal mass m and effective diameter σ. All pairs of particles in the system, except for the monomers and the flat surface, interact via a truncated Lennard-Jones (LJ) potential, which accounts for excluded volume effects:

$$U_{LJ}(r) = \begin{cases} 4\varepsilon\left[\left(\frac{\sigma}{r}\right)^{12} - \left(\frac{\sigma}{r}\right)^{6}\right] + \varepsilon\,, & r < r_c \\ 0\,, & r > r_c \end{cases}$$

Here, r is the distance between the particles, ε is a strength of the LJ interaction, and $r_c = 2^{1/6}\sigma$ is a cut-off distance. The parameter ε sets the energy scale of the system. Adjacent monomers are connected by a finitely extensible nonlinear elastic (FENE) spring potential defined by:[37]

$$U_{FENE}(r) = -\frac{1}{2}k_0 r_0^2 \ln\left[1 - \left(\frac{r}{r_0}\right)^2\right],$$

where $k_0 = 100(\varepsilon/\sigma^2)$ is a spring constant, and $r_0 = 1.5\sigma$ is the bond's maximum extension.

Furthermore, the attractive interaction between monomers and the flat surface contains a repulsive (excluded volume) part plus an attractive tail:

$$\begin{aligned} U_{mn}(r) &= \varepsilon\left[\left(\frac{\sigma}{r}\right)^{12} - 2\left(\frac{\sigma}{r}\right)^{6}\right] + \varepsilon - \varepsilon_b\,, \quad r < \sigma, \\ &= \varepsilon_b\left[\left(\frac{\sigma}{r}\right)^{12} - 2\left(\frac{\sigma}{r}\right)^{6}\right], \qquad r > \sigma, \end{aligned}$$

where ε_b is the potential well depth.

The Langevin equations of motion describing the dynamics of the chain were integrated using the velocity Verlet algorithm with a time step of dt = 0.002 τ, where $\tau = \sigma\sqrt{m/\varepsilon}$ is the LJ unit of time. The temperature was set at $T = \varepsilon/k_B$, where k_B is Boltzmann's constant.

3. Results & discussion

3.1. Which curvature is thermodinamically more favorable for the polymer-grafted nanoparticle?

Numerous studies have been previously carried out to understand the interaction between two polymer-graphed nanoparticles using self-consistent field theories and molecular dynamics simulations[38-40]. For two polymer-grafted particle systems in those studies, the repulsive steric force between polymer chains controls the interaction between the particles and prevent the particles from aggregation. However, in this study, the PGN is designed to adhere to the surface. In addition to the steric repulsive force between the polymer chains and the surface, we introduce Van der Waals attractions between them. The interplay between these two forces controls the adhesion strength between the PGN and the surface.

Preprints (www.preprints.org) | NOT PEER-REVIEWED | Posted: 23 February 2021 doi:10.20944/preprints202102.0505.v1

When the PGN approaches the surface and adheres to it due to the attractive interaction between the polymer chains and the surface, the conformation of the polymer chains changes. This new conformation dictates the contact surface area between the PGN and the surface, which consequently determines the adhesion strength. Depending on numerous parameters, including the polymer chains length, the strength of interaction between the polymer chains and the surface, and the geometry of the surface, this altered polymer conformation deviates from the corresponding conformation of a free PGN. In template-assisted self-assembly methods, porous materials are used to facilitate the assembly of colloids by favoring the pores to the flat part of the template[41]. However, it is not immediately obvious whether PGNs are more likely to bind to a flat surface or a curved one. In this section, we investigate the effect of surface curvature on the adhesion strength of the PGNs.

In order to illustrate how curvature of a surface can control the adhesion strength between the surface and a PGN, we study systems with the same PGN interacting with attractive surfaces having zero (flat), positive (hole) and negative (bump) curvatures (Fig. 1). We set the curvature of the convex and concave on the surface equal to $\pm 1/2$ of the curvature of the nanoparticle. This way, the convex and concave surfaces are curved enough to differ significantly from a flat surface, and the hole surface is spacious enough to accommodate the nanoparticle with grafted polymer chains. One measure for evaluating the binding strength between the PGN and a surface is the Potential Mean Force (PMF). We calculate it as a function of the separation distance between the center of the mass of the nanoparticles and the surface, by measuring the force between them at a given separation according to the following procedure.

(a)

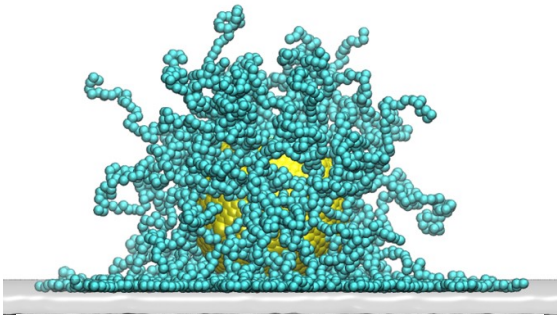

(b)

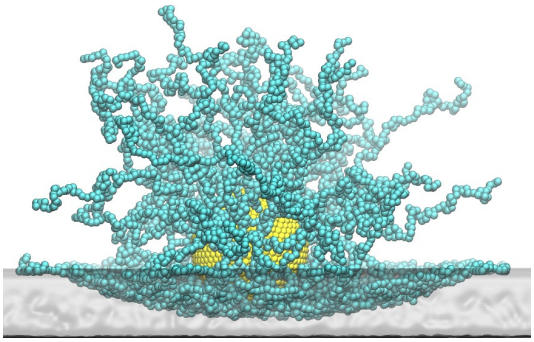

Preprints (www.preprints.org) | NOT PEER-REVIEWED | Posted: 23 February 2021 doi:10.20944/preprints202102.0505.v1

(c)

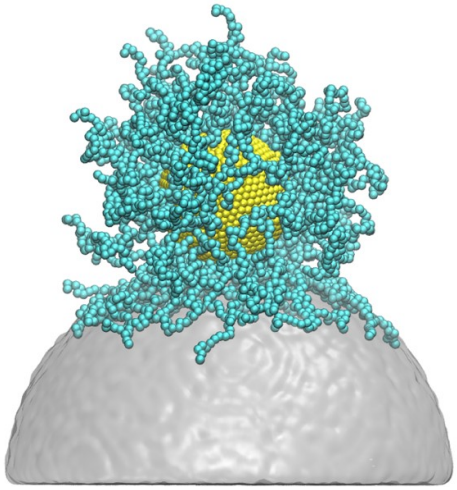

Figure 1. Snapshots of three systems of PGN interacting with the attractive substrates with: (**a**) zero (flat), (**b**) positive (hole), and (**c**) negative (bump) curvatures.

As noted above, the nanoparticle interacts with the surface only through the repulsive excluded volume force. The potential well depth of the LJ interaction between the polymer chains and the particles constructing the surfaces is set to $\varepsilon_b=3k_BT$. To ensure that the only changing parameters between the three systems is the curvature of the surface, we set the cut-off of the LJ potential to 2σ. Therefore, the polymer chains only interact with the particles of the surface which are located in the vicinity of them, not the ones outside of the curved area. After the equilibration stage is performed for the PGN, the immobile curved and flat surfaces consisting of close-packed spherical particles is introduced to each of the systems as shown in Fig. 1. These surfaces were placed in the vicinity of the nanoparticle, and the system was allowed to equilibrate again until the polymer chains adapt the curvature of the surface. Identical simulations were run for three surfaces with different curvatures. Using the equilibrated systems as starting points, 3x10=30 more systems, differing only in the distance of the surface to the center of the nanoparticle, with distances up to 20σ at intervals of 2, were analyzed. The center of the nanoparticle was approximately fixed to its initial coordinate by a permanent harmonic bond with the spring constant k=100. The force on the nanoparticle was calculated by observing the average displacement of the center of the nanoparticle from the initial coordinate, and then this was used as the displacement in a Hooke's Law equation. Next, the PMF was calculated by numerically integrating the force exerted by the spring on the nanoparticle along the direction perpendicular to the surface using the trapezoidal rule. Since the LJ potential is short-ranged, as we saw in our previous study[8], the PMF function decays to an asymptotic value (set to 0) as the distance between the nanoparticle and surface increases, and rises to a positive number at very short distances where repulsive steric effects dominate.

Preprints (www.preprints.org) | NOT PEER-REVIEWED | Posted: 23 February 2021 doi:10.20944/preprints202102.0505.v1

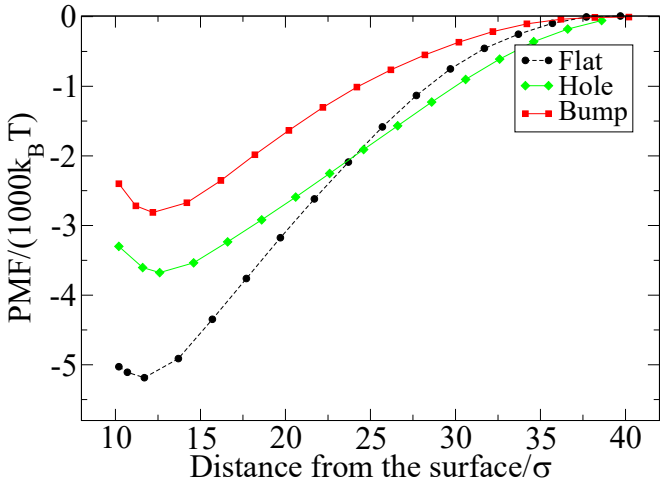

Figure 2. PMF of the nanoparticle center of mass as a function of distance from the surface for the systems with three different zero (flat), positive (hole) and negative (bump) curvatures.

As can be seen in Fig. 2, the system with the flat surface gives rise to the PMF with the deepest well, as compared to the convex and concave surfaces. Therefore, while it is thermodynamically more favorable for a bare nanoparticle to bind to the pores and concave surfaces due to a greater contact surface area as compared to flat and convex surfaces, the PGN is more likely to adhere to the flat surface[28, 35], all other parameters in the systems being the same. This result means that by tethering polymer chains to a nanoparticle, we can completely change its binding properties to surfaces with different geometries.

3.2. How does the rheology of polymer chains change upon seperation from the surface?

As mentioned earlier, the nanoparticle in our system is modeled as a rigid body. However, since the polymer chains that surround the nanoparticle are highly flexible, we can regard the PGN as a soft particle which deforms upon binding to the surface as its polymer chains spread to maximize its contact with the attractive surface and thus reduce the total energy of the system. Depending on the conformation and the potential applied between the interacting particles (i.e., polymer monomers) and the surface, the rheology of the polymer chains around the rigid nanoparticle may vary. In this subsection we see how the polymer chains' conformation changes upon separation from the curved and flat surfaces.

Preprints (www.preprints.org) | NOT PEER-REVIEWED | Posted: 23 February 2021 doi:10.20944/preprints202102.0505.v1

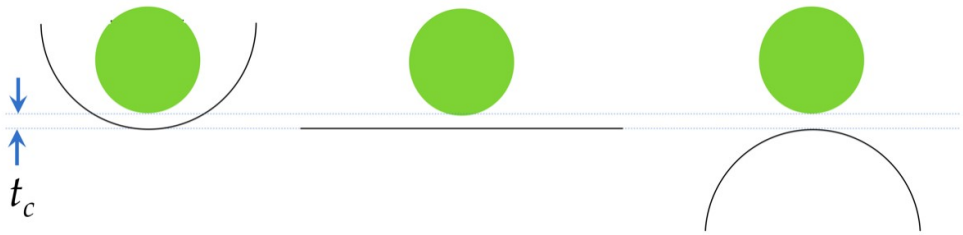

Figure 3. Schematic drawing of the nanoparticle on surfaces with positive, zero and negative curvatures. The region limited between two dotted lines shows the thickness of the layer consisting of polymer chains confined between the nanoparticle and the surface, t_c.

One of the parameters that describes this rheology is the thickness of the layer of polymer chains confined between the rigid nanoparticle and the surface (t_c), as shown in the schematic of Fig. 3. The measured thicknesses obtained by averaging over a long trajectory for three systems at equilibrium are shown in Table 1. As can be seen in Table 1, the smallest t_c corresponds to the flat surface, which has the deepest potential well among the three systems. On the other hand, the hole system has the thickest polymer layer confined between the nanoparticle and the surface. Comparison of t_c between the bump and hole systems tells us that a thinner polymer layer confined between the nanoparticle and surface does not necessarily imply stronger adhesion.

Another parameter that we have calculated for the equilibrium simulation is the mean value of the number of monomers in contact with the surface, n_c. While the flat surface shows the highest number of monomers in contact, the hole system with shallowest PMF well depth also possesses a high number of monomers in contact with the surface, which means n_c can be a good measure for the adhesion strength, as might be expected. Note that our attractive potential is short-range. For long-range interactions, the rheology of the polymer chains on the attractive surface might be different, and consequently the correlation between the PMF well depth and the n_c might not hold anymore.

Table 1. Parameters describing the rheology of polymer chains around the nanoparticle adhered to the surface with different curvatures. t_c is the thickness of the polymer chain layer confined between the rigid nanoparticle and surface, and n_c is the number of polymer monomers in contact with the surface. a_0 and a_s represent the surface areas of the interface between the PGN and the surfaces at equilibrium and upon separation, i. e. at the moment that the last particles belonging to the polymer chains detaches from the surface, for the flat and curved surfaces.

	Flat	Hole	Bump
t_c	1.2σ	2.1σ	1.7σ
n_c	2625	2460	1820
a_0	$1225\pi\sigma^2$	$1193\pi\sigma^2$	$1109\pi\sigma^2$
a_s/a_0	0.78	0.98	0.61

Fig. 4 shows the bottom view of our systems freely interacting under equilibrium condition. It can be seen that in the system with flat surface t_c is so small that in some snapshots of our equilibrium system, there are no monomers confined between the flat surface and the nanoparticle and the yellow surface of the nanoparticle is visible from the

Preprints (www.preprints.org) | NOT PEER-REVIEWED | Posted: 23 February 2021 doi:10.20944/preprints202102.0505.v1

bottom view. The surface area of the interface for the flat surface can be estimated as a circle and using $a_0 = \pi r_c^2$, where r_c is the approximate mean value of the radius of the contact area. For the other two systems with concave and convex surfaces, the surface areas of the interfaces can be estimated as sphere caps with the radius of r_c and depth/bump height of h_c which equals to $a_0 = \pi(r_c^2 + h_c^2)$. As can be seen in Table 1, and as expected, a_0 shows the same trend as n_c with the PMF well depth.

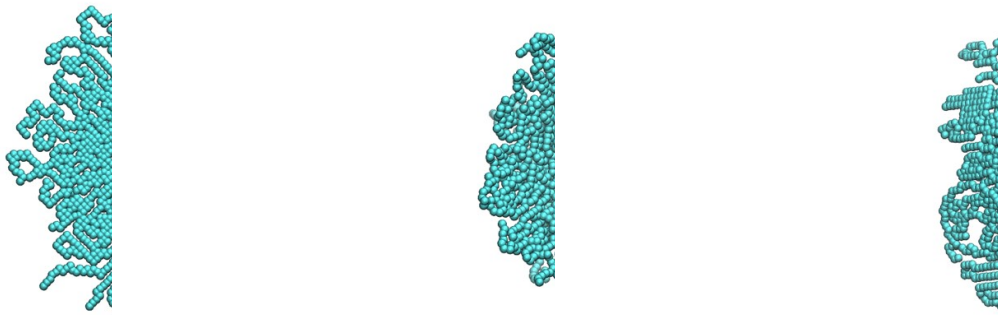

Figure 4. Bottom view of the PGN in contact with flat, concave and convex rigid surfaces (from left to right). The surface area accessed by the polymer chains is different for each system, which affects the number of interacting particles and consequently the adhesion strength.

To further investigate the relationship between the adhesion strength and the rheology of polymer chains, we simulate the separation of PGN from the surface by applying an external pulling force on the nanoparticle. The applied force was increased at a constant rate of $0.0028 k_B T/\sigma\tau$ on the center of mass of the nanoparticle. We continue the simulation until the nanoparticle is completely separated from the surface. Fig. 5 shows the applied force versus the displacement of the nanoparticle's center of mass for our three systems. As is evident from the figure, by increasing the pulling force, the distance between the PGN and the surface gradually grows until at some critical force the PGN suddenly jumps apart from the interacting surface. This behavior has been also predicted by The Johnson–Kendall–Roberts (JKR) theory[42, 43]. This model describes how two elastic bodies adhere together and what deformation they undergo when in contact with each other. To see how accurate this theory predicts the separation threshold, we calculate the surface area of the interface between the PGN and the surface at the point where they separate. For a flat surface, the JKR theory predicts that separation occurs abruptly once the contact surface area reaches to a_s/a_0=0.4. We also observe this abrupt separation in our pulling simulation, however, according to our results shown in Table 1, this number is ~0.78. This discrepancy reflects the intrinsic differences between the elastic sphere interacting with a rigid surface assumed in the JKR theory and our PGN. For instance, as one can see in Fig. 4, the boundaries of the contact regions are diffuse and fluid-like, while JKR theory assumes that the boundaries are sharp and well-defined. This result tells us that the JKR theory cannot predict the rheological behavior of the PGNs quantitatively and numerical methods provide more accurate information about this system.

Preprints (www.preprints.org) | NOT PEER-REVIEWED | Posted: 23 February 2021 doi:10.20944/preprints202102.0505.v1

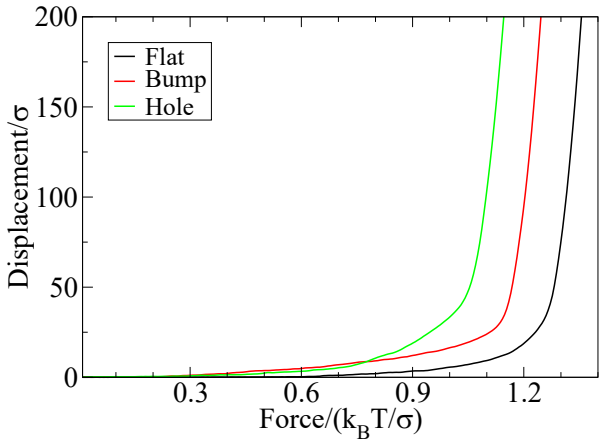

Figure 5. Force versus displacement of the center of mass of the nanoparticle for three systems under external force. The force increases at the same rate for our three systems. The sudden increase of displacement determines where the separation of the deformable polymer-grated nanoparticles from the rigid attractive surface occurs. While according to the results depicted in Fig. 2, the adhesion of the nanoparticle to the surface with the hole is stronger than the surface with the bump, due to the conformation of polymer chains confined between the nanoparticle and surface, the separation occurs at a smaller force for the nanoparticle on the hole.

Another interesting observation one can make comparing Fig. 5 and 2 is that while the system with convex surface shows the shallowest energy well among other systems, the smallest separation force corresponds to the system with concave surface. The reason that the hole system shows a bigger displacement at a smaller force comparing to the other two systems may be the thick layer of polymer chains confined between the surface and the nanoparticle, t_c. Since the monomers contributing in that layer are not adhered to the surface, they do not resist against the applied pulling force. As a result, the displacement grows quickly up to the point that the PGN completely separates from the surface. Different methods for separating the PGN from the surface, such as applying displacement with a constant rate, might result in a different separation onset behavior among our systems.

4. Conclusion

Adhesion of a PGN to attractive surfaces with zero, positive and negative curvatures was evaluated using CGMD. According to the calculated PMFs, the flat surface shows the strongest, and the convex surface shows the weakest adhesion to the PGN. Moreover, we studied the separation of PGN from surfaces by applying an external pulling force to the PGN. Our results agreed qualitatively with the JKR theory prediction. It may be possible to exploit the results presented here can be exploited in drug delivery and self-assembly applications.

Author Contributions: Conceptualization, R.D.C., A.O. and M.O.; methodology, M.O. and R.D.C; simulation and visualization, A.O and M.O.; validation, R.D.C. and M.O.; writing, R. D. C, A.O. and M.O.;

All authors have read and agreed to the published version of the manuscript.

Funding: This research received no external funding.

Data Availability Statement: The data presented in this study are available on request from the corresponding author.

Acknowledgments: The authors acknowledge the Texas Advanced Computing Center (TACC) at The University of Texas at Austin for providing HPC resources that have contributed to the research results reported within this paper. URL: http://www.tacc.utexas.edu. RDC acknowledges the support of NSF grant CHE 1954865.

Conflicts of Interest: The authors declare no conflict of interest.

References

1. A. Firouzeh, M. Ozmaeian and A. Alasty, Smart Materials and Structures **21** (6), 065011 (2012).
2. S. K. Kumar, B. C. Benicewicz, R. A. Vaia and K. I. Winey, Macromolecules **50** (3), 714-731 (2017).
3. S. K. Kumar, N. Jouault, B. Benicewicz and T. Neely, Macromolecules **46** (9), 3199-3214 (2013).
4. B. Wang, B. Li, B. Dong, B. Zhao and C. Y. Li, Macromolecules **43** (22), 9234-9238 (2010).
5. P. Akcora, H. Liu, S. K. Kumar, J. Moll, Y. Li, B. C. Benicewicz, L. S. Schadler, D. Acehan, A. Z. Panagiotopoulos, V. Pryamitsyn, V. Ganesan, J. Ilavsky, P. Thiyagarajan, R. H. Colby and J. F. Douglas, Nat Mater **8** (4), 354-359 (2009).
6. K. Ohno and Y. Mizuta, ACS Applied Polymer Materials **2** (2), 368-375 (2019).
7. A. Walther and A. H. Muller, Chemical reviews **113** (7), 5194-5261 (2013).
8. M. Ozmaian, B. A. Freitas and R. D. Coalson, The Journal of Physical Chemistry B **123** (1), 258-265 (2018).
9. G. Fritz, V. Schädler, N. Willenbacher and N. J. Wagner, Langmuir **18** (16), 6381-6390 (2002).
10. W. B. Russel, W. Russel, D. A. Saville and W. R. Schowalter, *Colloidal dispersions*. (Cambridge university press, 1991).
11. J. Hu, W. Tang, Y. Li, J. He, X. Guo and R. Yang, Polymers **12** (2), 278 (2020).
12. S. Chandran, N. Begam and J. Basu, Journal of Applied Physics **116** (22), 222203 (2014).
13. K. P. Santo, A. Vishnyakov, Y. Brun and A. V. Neimark, Langmuir **34** (4), 1481-1496 (2018).
14. M. A. Stuart, W. T. Huck, J. Genzer, M. Muller, C. Ober, M. Stamm, G. B. Sukhorukov, I. Szleifer, V. V. Tsukruk, M. Urban, F. Winnik, S. Zauscher, I. Luzinov and S. Minko, Nat Mater **9** (2), 101-113 (2010).
15. N. Kamaly, G. Fredman, J. J. R. Fojas, M. Subramanian, W. I. Choi, K. Zepeda, C. Vilos, M. Yu, S. Gadde and J. Wu, ACS nano **10** (5), 5280-5292 (2016).
16. S. de Beer, E. Kutnyanszky, P. M. Schon, G. J. Vancso and M. H. Muser, Nat Commun **5**, 3781 (2014).
17. D. A. Walker, E. K. Leitsch, R. J. Nap, I. Szleifer and B. A. Grzybowski, Nat Nanotechnol **8** (9), 676-681 (2013).
18. E. Gonzalez Solveyra and I. Szleifer, Wiley Interdisciplinary Reviews: Nanomedicine and Nanobiotechnology **8** (3), 334-354 (2016).
19. H. Lu, J. Su, R. Mamdooh, Y. Li and M. H. Stenzel, Macromolecular Bioscience **20** (1), 1900221 (2020).
20. N. Bachhar, Y. Jiao, M. Asai, P. Akcora, R. Bandyopadhyaya and S. K. Kumar, Macromolecules **50** (19), 7730-7738 (2017).
21. R. M. Choueiri, E. Galati, H. Therien-Aubin, A. Klinkova, E. M. Larin, A. Querejeta-Fernandez, L. Han, H. L. Xin, O. Gang, E. B. Zhulina, M. Rubinstein and E. Kumacheva, Nature **538** (7623), 79-83 (2016).
22. X. Liang, R. Dong and J. C. Ho, Advanced Materials Technologies **4** (3) (2019).
23. M. Ozmaian, A. Fathizadeh, M. Jalalvand, M. R. Ejtehadi and S. M. Allaei, Sci Rep **6**, 21910 (2016).
24. S. E. Creager, L. A. Hockett and G. K. Rowe, Langmuir **8** (3), 854-861 (1992).
25. A. Rasmuson, E. Pazmino, S. Assemi and W. P. Johnson, Environ Sci Technol **51** (4), 2151-2160 (2017).
26. C. Shen, L.-P. Wang, B. Li, Y. Huang and Y. Jin, Vadose Zone Journal **11** (1) (2012).
27. S.-Y. Zhang, M. D. Regulacio and M.-Y. Han, Chemical Society Reviews **43** (7), 2301-2323 (2014).
28. R. van Dommelen, P. Fanzio and L. Sasso, Adv Colloid Interface Sci **251**, 97-114 (2018).
29. Y. H. Ye, S. Badilescu, V.-V. Truong, P. Rochon and A. Natansohn, Applied Physics Letters **79** (6), 872-874 (2001).
30. M. Perez-Page, E. Yu, J. Li, M. Rahman, D. M. Dryden, R. Vidu and P. Stroeve, Adv Colloid Interface Sci **234**, 51-79 (2016).

31. L. Wang, J. Ma, W. Hong, H. Zhang and J. Lin, Macromolecules **53** (19), 8393-8399 (2020).
32. M. J. A. Hore, L. T. J. Korley and S. K. Kumar, Journal of Applied Physics **128** (3) (2020).
33. K. R. Medidhi and V. Padmanabhan, J Chem Phys **150** (4), 044905 (2019).
34. X. Yong, Langmuir **31** (42), 11458-11469 (2015).
35. S. Sacanna, W. T. Irvine, P. M. Chaikin and D. J. Pine, Nature **464** (7288), 575-578 (2010).
36. S. Plimpton, Journal of computational physics **117** (1), 1-19 (1995).
37. G. S. Grest, K. Kremer and T. Witten, Macromolecules **20** (6), 1376-1383 (1987).
38. S. Goyal and F. A. Escobedo, J Chem Phys **135** (18), 184902 (2011).
39. J. U. Kim and M. W. Matsen, Macromolecules **41** (12), 4435-4443 (2008).
40. D. Trombly and V. Ganesan, Journal of Polymer Science Part B: Polymer Physics **47** (24), 2566-2577 (2009).
41. S. Ni, J. Leemann, I. Buttinoni, L. Isa and H. Wolf, Science advances **2** (4), e1501779 (2016).
42. K. L. Johnson, K. Kendall and a. Roberts, Proceedings of the royal society of London. A. mathematical and physical sciences **324** (1558), 301-313 (1971).
43. J. N. Israelachvili, *Intermolecular and surface forces*. (Academic press, 2011).